Viscoelastic behaviour of polycaprolactone/clay nanocomposites

L Ludueña, A Vazquez and V Alvarez

Journal of Composite Materials published online 3 August 2011
DOI: 10.1177/0021998311410476

Article

JOURNAL OF COMPOSITE MATERIALS

Journal of Composite Materials
0(0) 1–13

DOI: 10.1177/0021998311410476
jcm.sagepub.com

SAGE

Viscoelastic behavior of polycaprolactone/clay nanocomposites

L. Ludueña[1], A. Vázquez[2] and V. Alvarez[1]

Abstract

The creep behavior of polycaprolactone and polycaprolactone/clay nanocomposites prepared by melt intercalation was studied. Sodium montmorillonite and organo-modified montmorillonite were used as reinforcement in order to analyze the effect of clay dispersion degree. Both a viscoelastic creep model named Burgers (four parameters) and an empirical method called Findley power law were applied to fit the experimental data (elastic, primary creep stage, and secondary creep stages). An additional effort was conducted to relate the parameter analysis of the Burgers model with the experimental behavior at each creep stage. The variation of the theoretical parameters illustrated the influence of the nanofillers on the experimental creep performance of the bulk matrix. Time–temperature superposition principle was used to predict the long-term behavior based on the short-term experimental data. The Findley power law model was also employed to reproduce the master curves. Both experimental curves and models demonstrated that the incorporation of the clay produces a significant improvement on the creep resistance at short times. This effect was higher for the best-dispersed nanocomposite. The latter result was strictly related to the great enhancement of the elastic behavior since in that case the time-dependent deformations were higher than those of the neat matrix.

Keywords

nanocomposites, clay, dispersion, creep, rheology

Introduction

Due to waste accumulation of traditional polymeric products at the end of the life cycle, the development of environmental friendly and biodegradable, polymeric materials have attracted extensive interest.[1] Polycaprolactone (PCL) is a chemically synthesized polymer based on caprolactone units, which does not occur in nature but it is fully biodegradable.[2]

In order to obtain a competitive product, the PCL performance can be greatly enhanced with the addition of nanometer-size inorganic fillers to produce nanocomposites that have the interesting characteristics such as mechanical properties;[3] barrier properties;[4] thermal properties,[5] and some others such as the flammability,[6] water adsorption,[7] and creep resistance,[8] which can be greatly enhanced with the addition of a small amount of filler (usually less than 10 wt%).[1–8]

One kind of nanometer-size reinforcement is montmorillonite, which is a layered silicate whose interlayer ions can be exchanged by organo-ions in order to produce an increment in the interlayer spacing ($d_{0\,0\,1}$) and to improve the polymer/clay compatibility. These improvements are important in order to increase the dispersion degree of clay platelets in the polymeric matrix.[9]

The characterization of the clay morphology inside the nanocomposite is crucial to understand this kind of materials. Exfoliated structures, where the individual clay platelets are randomly and uniformly dispersed into the polymer matrix, and intercalated structures, where the polymer chains are intercalated between the silicate layers, are the morphologies of this class of

[1]Research Institute of Material Science and Technology (INTEMA), Engineering Faculty, National University of Mar del Plata, Mar del Plata, Argentina.
[2]INTECIN (UBA-CONICET), Polymer and Composite Group, Engineering Faculty, University of Buenos Aires, Buenos Aires, Argentina.

Corresponding author:
V. Alvarez, Research Institute of Material Science and Technology (INTEMA), Engineering Faculty, National University of Mar del Plata, Juan B. Justo 4302, (B7608FDQ) Mar del Plata, Argentina
Email: alvarezvera@fi.mdp.edu.ar

nanocomposites. Generally, both clay structures are present when the morphology of a polymer/clay nanocomposite sample is microscopically analyzed.[10] Several characterization techniques can be used to analyze the dispersion degree of the clay inside a polymer matrix:[11] X-ray diffractometry (XRD) is one of these methods, which is useful to measure how the interlayer distance of the clay becomes higher as the polymer chains intercalate inside the clay galleries. When the interlayer distance becomes higher, or the intercalation of the polymer is more effective, the diffraction peak corresponding to the clay alone shifts toward lower angles up to the clay diffraction peak is not visible any more. Intercalated structures may have interlayer distances higher than 4 nm but the typical instruments have resolutions lower than 4 nm (corresponding to the complete disappearance of the clay diffraction peak), so this technique is deficient to characterize fully exfoliated nanocomposites.[11] Transmission electron microscopy (TEM) is another technique used to observe the morphology of clay platelets in a polymeric matrix. However, the extremely high resolution of this method allows evaluating only very small regions ($\sim 8\ \mu m^2$) of the material which may not be representative of the total nanocomposite. On the other hand, the preparation of the samples is difficult, the technique is costly to be used as routine test, and several specimens must be evaluated to have a complete characterization.[11]

An interesting alternative to analyze effects of compatibilizer on the interfacial interactions and clay dispersion in the molten polymer phase is the melt rheology. Several authors have found that the melt rheology is strongly influenced by nanoparticles.[12–15] Exfoliated or well-dispersed nanocomposites often show a pseudo-solid-like rheologic behavior at low shear rates with a pronounced shear thinning behavior of the bulk polymer.[15] The reasons for these results are not completely understood.[13] While Zhao et al.[15] proposed that the solid-like behavior observed for highly dispersed nanocomposites is a consequence of the increment of the rate of change of clay orientation under flow, Sung et al.[16] explained that it is produced by the incapacity of the clay platelets to freely rotate under flow (the opposite explanation), and Wagener et al.[17] attributed this phenomenon by the fact that when the clay is well-dispersed the probability to occur edge to face and edge to edge interactions is increased, which may build and mechanically stabilize mesoscale rigid structures known as card-house inhibiting the polymer chain movement under shear flow. Even so, all authors[15–17] concluded that the pronounced shear thinning behavior at low shear rates is an indication of better clay dispersion degree inside the matrix. This method has the advantages that the information obtained is representative of the whole sample instead of small zones of it and samples do not need to be specially conditioned.

Plastic products support constant stresses for long periods of time mostly during its storage, so that the study of the deformation processes along time under a constant stress becomes relevant. Polymers are viscoelastic in nature; thus, the deformation behavior is not only temperature-dependent but also time-dependent. The time-dependent deformation of materials subjected to a constant stress is called creep.[18] Several authors have studied and modeled[18–23] the creep behavior of polymer/clay nanocomposites showing that nanoparticles can improve the creep resistance of different matrices as far as total dispersion of the clay platelets (exfoliation) is achieved.[19–21] Chiou et al.[23] have evaluated the creep behavior of starch–clay nanocomposites with several clays; they have confirmed that the decrease on the creep compliance was related to the polymer–clay interaction; which was higher in the case of higher compatibility. This is an evidence of the more effective reinforcement effect as far as total dispersion of the clay platelets (exfoliation) is achieved.

Yang et al.[18] have modeled the creep behavior of polyamide 66 nanocomposites whose experimental results were obtained in a previous work.[8] They have demonstrated that both the constitutive Burgers model and the empirical Findley power law could satisfactorily describe the creep strain and creep rate showing that the Findley power law was good for predicting over large time scale. The master curves constructed using the time–temperature superposition principle (TTSP) greatly extended the creep behavior over 11 decades of time. In addition, the Findley power law parameters also showed that the creep resistance of the nanocomposites was clearly improved compared to that of neat matrix. Pérez et al.[22] have studied the creep behavior of PCL/starch blends and its nanocomposites with organo-modified layered silicate. They have demonstrated that the creep compliance decreased by the incorporation of clay relating this effect to the enhancement of the modulus. In addition, it was shown that the parameters of Burgers model confirmed this trend: the instantaneous and retardant modulus increased and the permanent viscosity and relaxation time decreased as a function of clay content, and the efficiency of nanofillers to achieve better creep performance of neat matrix was confirmed by the parameters of the Findley power law model which properly represented the real strain–time curves of matrix and nanocomposites in the selected range of temperatures. The master curves displayed a tolerable superposition and the activation energy for the shift factor was also an evidence for the creep resistance development. Nevertheless, in that case, only one organo-modified

clay was employed, so that it was not possible to make comparisons regarding the dispersion degree.

The aim of this study was to establish the effect of clay dispersion on the viscoelastic behavior of PCL/clay nanocomposites. For this purpose, different clays were used and the effect of the clay/polymer compatibility on the creep behavior was experimentally analyzed and mathematically modeled. The morphology of the clay inside the nanocomposites was characterized by different techniques in order to establish a correlation between the creep behavior and the clay dispersion degree. It must be noted the importance of this study since the matrix is a biodegradable polymer that can be processed with traditional industrial machines[3] and the clay is a cheap and easily available filler that can produce great improvements on a wide range of properties.

Theoretical background

Rheological characterization

The melt rheology curves were fitted to the power law expression:

$$\eta = A_{\mathrm{Rh}} \cdot \dot{\gamma}^{(n_{\mathrm{Rh}})} \tag{1}$$

where the subscript Rh represents a rheology parameter, η the dynamic viscosity; A_{Rh} a preexponential factor; $\dot{\gamma}$ the shear rate and n_{Rh} the shear thinning exponent. In the double logarithmic plot, a linear zone at low shear rates can be seen (solid lines shown in Figure 1). The n_{Rh} parameter was calculated from slope of this region.[17] Regarding polymer/clay nanocomposites, several authors[15,17,24,25] have found that the n_{Rh} value is higher as the clay dispersion degree is improved.

Experimental creep behavior

The creep behavior (expressed as deformation, ε, along time, t) of polymers consists in four stages, namely (1) instantaneous deformation, ε_0, (2) primary creep, $\varepsilon_1 - \varepsilon_0$, (3) secondary creep, $\varepsilon_2 - \varepsilon_1$, and (4) tertiary creep, $\varepsilon_3 - \varepsilon_2$ (Figure 2 (a)). When external load is applied, the material responds with an instantaneous strain ε_0 (independent of time) due to the elastic or plastic deformation of the polymer. Then, the creep rate, $d\varepsilon/dt$, starts at a relatively high value, which decreases rapidly with time and may result from the slippage and orientation of polymer chains under persistent stress (primary creep stage, $[\varepsilon_0,0; \varepsilon_1,t_1]$). After a certain period of time, the creep rate reaches a steady-state value in the secondary creep stage ($[\varepsilon_1,t_1; \varepsilon_2,t_2]$), in which the viscoelastic flow in the polymer occurs. Finally, the material falls into the tertiary creep stage, where the creep rate increases rapidly and final creep rupture or advanced necking occurs ($[\varepsilon_2,t_2; \varepsilon_3,t_3]$).[26]

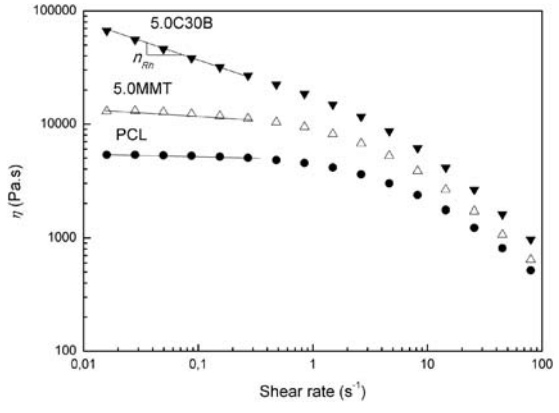

Figure 1. Dynamic viscosity, η, as a function of shear rate for PCL and nanocomposites.
Note: Points represent experimental values and lines the power law fitting.

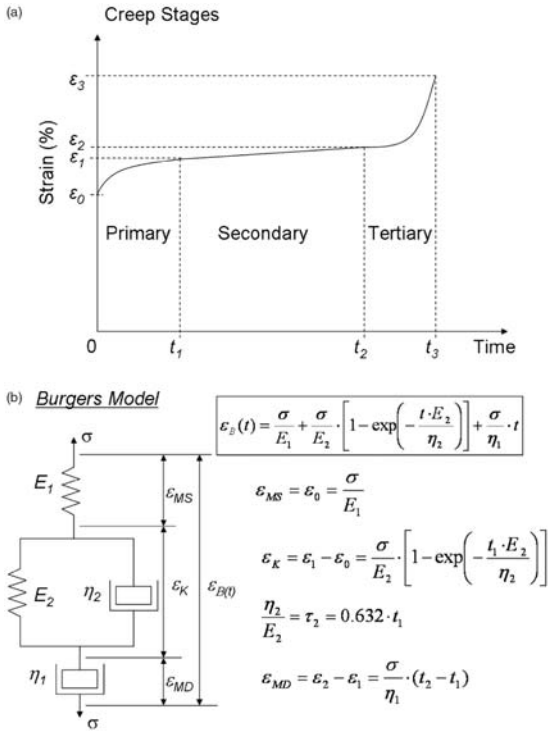

Figure 2. Scheme of: (a) the creep stages and (b) characteristic strains of the Burgers model and their relation with the experimental behavior.

Creep models

Four-element model. The variation of the theoretical parameters of the four-element or Burgers model,[27] helps to better understand the influence of the nanofillers on each stage of the creep behavior. This model is a series combination of the Maxwell and Kelvin–Voigt models.[28] The total strain $\varepsilon_B(t)$ is given by the general equation:

$$\varepsilon_B(t) = \varepsilon_{MS} + \varepsilon_K + \varepsilon_{MD} \quad (2)$$

where ε_{MS} and ε_{MD} are the elastic and viscous strains corresponding to the spring and dashpot of the Maxwell model and ε_K the viscoelastic strain represented by the Kelvin–Voigt unit. The creep deformation in the Burgers model can be finally written as:[29]

$$\varepsilon_B(t) = \frac{\sigma}{E_1} + \frac{\sigma}{E_2} \cdot \left[1 - \exp\left(-\frac{t \cdot E_2}{\eta_2}\right)\right] + \frac{\sigma}{\eta_1} \cdot t \quad (3)$$

where E_1 and E_2 are the elastic moduli, η_2 and η_1 the viscosities, σ the applied stress, and t the time while the constant load is applied. This model has only one retardation time, $\tau_2 = \eta_2/E_2$. This time is defined as the time needed to produce 63.2% ($1 - e^{-1}$) of the total deformation in the Kelvin unit. Figure 2(b) shows a scheme of the Burgers model and the relationship between the deformations of each unit and the experimental creep stages. When the constant load is applied, the initial instantaneous elastic deformation, ε_{MS}, takes place in the spring. Later deformation, ε_K, is related to the primary creep stage and comes from the spring E_2 and dashpot η_2. It represents the delayed elastic deformation of the Kelvin unit. The deformation associated to the secondary creep stage, ε_{MD}, is a time-dependent viscous flow and comes from the Maxwell dashpot with the viscosity η_1. When the load is removed, the creep deformation is all recoverable except for the flow that occurred in that dashpot (ε_{MD}). The tertiary creep stage will not be experimentally analyzed, because it requires longer times, and it is not taken into account in the Burgers model.

Four-element model can be used to satisfactorily model the creep behavior of viscoelastic materials. The effect of nanofillers can be determined from the variation of the model parameters E_1, E_2, η_1, and τ_2 that can be obtained from experimental data.

Differentiating Equation (3), the creep rate of the Burgers' model, $\dot{\varepsilon}_B$, can be obtained:[22]

$$\dot{\varepsilon}_B(t) = \frac{\sigma}{\eta_1} + \frac{\sigma}{\eta_2} \cdot \exp\left(-\frac{t \cdot E_2}{\eta_2}\right) \quad (4)$$

When long creep times are analyzed, the creep rate reaches a constant value given by: $\dot{\varepsilon}_B(\infty) = \frac{\sigma}{\eta_1}$.

Findley power law model

The viscoelastic behavior of thermoplastic composites has been modeled using an empirical model based on a power law equation known as Findley model;[30] that can be expressed as follows:

$$\varepsilon_{PL}(t) = \varepsilon_0 + A \cdot t^{n_{PL}} \quad (5)$$

where the subscript PL indicates that the parameter is associated with the power law model, $\varepsilon_{PL}(t)$, is the creep strain at time, t, ε_0 is the initial instantaneous strain, A the amplitude of transient creep strain, and n_{PL} the time exponent. The instantaneous strain, the amplitude of transient creep strain, and the time exponent are known as creep parameters. The relative creep strain, ε_r, is defined as the ratio between the creep strain value at each time, $\varepsilon(t)$, and the instantaneous initial strain, ε_0. Rearranging the Equation (5), the relative creep strain can be expressed as:

$$\varepsilon_r = 1 + A' \cdot t^{n_{PL}} \quad (6)$$

where

$$A' = \frac{A}{\varepsilon_0}.$$

Differentiating Equation (5), it is possible to obtain the power law creep rate, i.e., $\dot{\varepsilon}_{PL}$, as follows:

$$\dot{\varepsilon}_{PL} = \frac{n_{PL}.A}{t^{1-n_{PL}}} \quad (7)$$

It must be noted that when $t \to \infty$, $\dot{\varepsilon}_{PL} \to 0$. This case is true only for polymers that do not exhibit a pronounced secondary creep stage. This model allows predicting with good accuracy the viscoelastic behavior over a wide time scale.[30]

Master curves

Long-term creep predictions can be estimated from the data acquired in short-time tests. For this purpose, TTSP can be used. This method establishes that, in the linear-viscoelastic regime, creep curves at two different temperatures can be superposed changing the time scale by applying a shift factor, a_T, at a reference temperature T_r. If T_r is far away from the glass transition temperature of the material, the dependence of the shift factor with the temperature can be described by an Arrhenius type equation:[31]

$$\log a_T = \frac{Q}{2.303 \cdot R} \cdot \left(\frac{1}{T} - \frac{1}{T_r}\right) \quad (8)$$

where Q is the activation energy, R the universal gas constant and T the temperature of the creep test.

Creep compliance, $J(t)$, is another important parameter that can be used to describe the creep behavior and it is defined as follows:

$$J(t) = \frac{\varepsilon(t)}{\sigma} \tag{9}$$

Findley power law can be also applied at this stage to correlate the experimental creep compliance with time at the reference temperature as shown in the following equation:

$$J_{PL}(t) = J_{PL0} + J_{PL1} \cdot t^{n_{MC}} \tag{10}$$

where the subscript MC indicates a parameter associated with the master curves, n_{MC} is the time exponent, J_{PL0} is the time-independent compliance and J_{PL1} is the time-dependent term.

Experimental

Materials

The matrix used in this study was a commercial PCL (Mn 80000), supplied by Sigma–Aldrich. Two different clays, commercially named Cloisite Na (MMT) and Cloisite 30B (C30B), purchased from Southern Clay Products Inc., were used as received as nanofillers. The characteristics of the clays are given in Table 1.

Composite preparation

Nanocomposites with 5 wt% of each clay, called 5.0C30B and 5.0MMT, were prepared by melt-intercalation followed by compression-molding. In previous works[3,32] the effect of C30B content on the clay morphology; thermal and mechanical properties was studied concluding that 5 wt% of this clay lead to the best performance. An intensive Brabender type mixer with two counter-rotating roller rotors was used. Mixing temperature was 100°C; speed of rotation was 150 rpm and mixing time was 10 min. Compression molding was carried out in a hydraulic press for 10 min at 100°C. The thickness of the samples was in the range of 0.3-0.5 mm.

Table 1. Characteristics of clays used as nanofillers

Material	Organic modifier	Modifier concentration (meq/100 g clay)
Cloisite Na (MMT)	None	–
Cloisite 30B (C30B)	CH_2CH_2OH H_3C—N+—T CH_2CH_2OH	90

HT, hydrogenated tallow (~65% C18; ~30% C16; ~5% C14).

Methods

- XRD patterns were recorded by a PW1710 diffractometer equipped with an X-ray generator ($\lambda = 0.154060$ nm). Samples were scanned in 2θ ranges from 3° to 60° by a step of 0.035°.
- TEM micrographs were taken with a JEOL JEN 1220 operated at 100 kV in the bright field mode. Ultrathin sections (~50 nm) of the samples were cut at −120°C using a Leica UCT ultramicrotome equipped with a diamond knife.
- Rheology analysis was conducted in a Rheometric Scientific Ares rheometer under nitrogen atmosphere. Plate–plate geometry with a plate diameter of 25 mm was used. Samples were inserted and heated to 80°C. Low shear amplitude (2%) was used in order to avoid the destruction of any stabilized clay structure and to work in the linear viscoelastic regime. Data were taken for shear rates in the range 0.1–100 s^{-1}.
- Tensile tests were performed in a universal testing machine Instron 4467 at a constant crosshead speed of 50 mm/min. Before tests, all specimens were preconditioned at 65% RH (relative humidity) and room temperature.
- Flexural creep behavior was studied using a DMA 7-e Perkin Elmer under nitrogen atmosphere. Tests were carried out at different temperatures from 16°C to 28°C, all of them above the glass transition temperature of the matrix (–60°C). The temperature accuracy of the equipment was ±1°C. Previously, several stresses were tested in order to work in the linear viscoelastic regime; selecting 8 MPa to be applied for 30 min and then it was removed.

Results and discussion

Clay morphology

Figure 3 shows XRD patterns for clay and nanocomposites. The clay diffraction peak shifted toward lower angles for 5.0MMT while it disappeared for 5.0C30B;

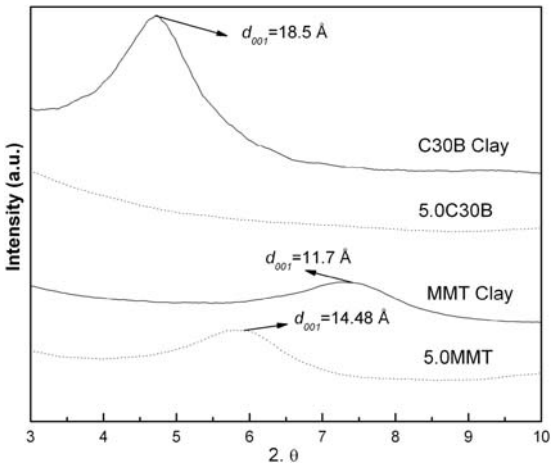

Figure 3. X-ray diffractograms for the clays used and PCL/clay nanocomposites.

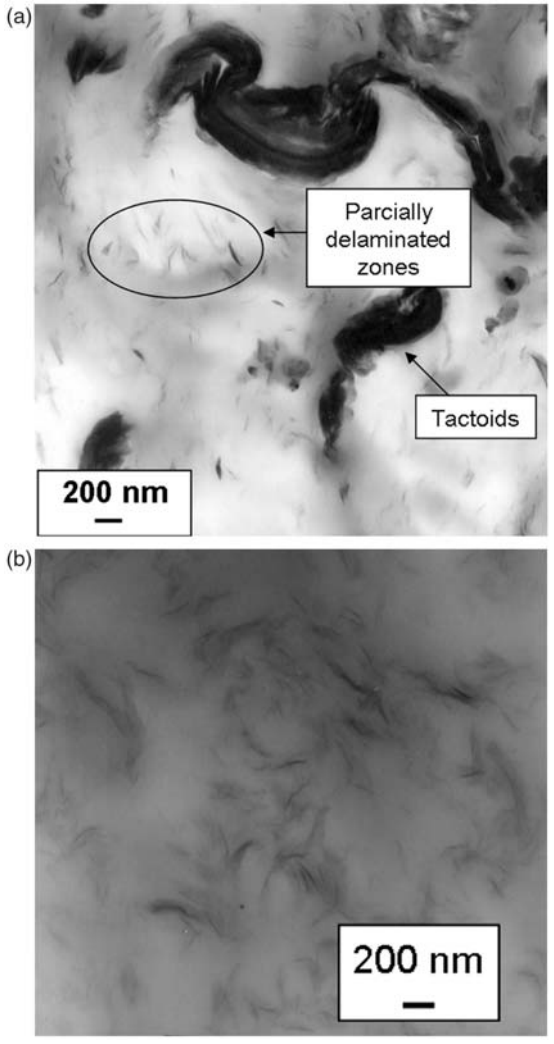

Figure 4. TEM micrographs of: (a) MMT and (b) C30B nanocomposites.

which indicates that the compatibilized montmorillonite was intercalated at a higher degree.

TEM micrographs of nanocomposites are shown in Figure 4(a) and (b). TEM images where converted into black and white by printing them on a paper and tracing over in a transparent film with a permanent marker. The obtained pictures were then scanned in order to be analyzed by adequate software (Image Pro Plus). TEM pictures are obtained in a gray scale and low contrast; therefore, it is possible to statistically measure the different clay arrangements (agglomerated, intercalated, and delaminated zones) by this procedure. Figure 4(a) is representative of MMT nanocomposite. The dark zones are silicate platelets and so it is evident the presence of MMT agglomerates of around 600 nm and some other intercalated areas with separations between the platelets of less than 2–3 nm and a number of platelets per particle of 3 ± 2. This result may be a consequence of low compatibility between the clay and the matrix, where tactoids or intercalants are obtained and only a partial or no exfoliation can occur. In the case of the nanocomposite with C30B (Figure 4(b)), a mixed intercalated–exfoliated structure was observed. Areas with delaminated particles and smaller aggregates of around 200 nm were found. In this case, the average number of platelets per particle was 2 ± 1. The chemical modification of C30B improves the dispersion degree since the clay surface becomes more hydrophobic and hence more compatible with the matrix (because PCL is strongly hydrophobic). This modification also produces an increment in the interlayer spacing facilitating the intercalation process.[33] These results are in accordance with those of XRD.

Figure 1 shows the apparent viscosity, η, as a function of the shear rate, $\dot{\gamma}$, for the matrix and nanocomposites (PCL, 5.0MMT and 5.0C30B). PCL and 5.0MMT showed a Newtonian behavior at low shear rate, with higher viscosity for 5.0MMT as a result of the impedance of the polymer chains to flow around the rigid MMT particles, while the 5.0C30B nanocomposite showed a pseudo-solid-like behavior with pronounced shear thinning (higher n_{Rh}, Table 2). It is clear the tendency of higher n_{Rh} for the nanocomposite with the best clay dispersion degree. The same trend was found by other authors[15,17,24,25] for similar thermoplastic/clay systems.

Experimental creep behavior

Figure 5(a) shows the deformation along time for the 5.0C30B nanocomposite at different temperatures. The shape of the curves did not change with the temperature for all materials analyzed. The matrix becomes softer as the temperature is raised; thus, regarding the same stress level and creep time, the creep strain will be

Table 2. Parameters at 25°C for PCL and their clay nanocomposites obtained by: clay dispersion analysis (XRD, TEM, rheology), static tensile tests, experimental creep analysis, creep models (Burgers, Findley power law), and experimental and modeled creep rates and master curves modeling.

Material	Polymer/clay compatibility	Clay dispersion	$-n_{Rh}$	E (MPa)	ε_0 (%)	$\varepsilon_1-\varepsilon_0$ (%)	$\varepsilon_2-\varepsilon_1$ (%)	ε_f (%)	E_1 (MPa)	E_2 (MPa)	τ_2 (s)	η_1 (GPa·h)	A' (10^{-4} $s^{-n_{PL}}$)	$\dot{\varepsilon}_{Experimental}$ (10^{-7} s^{-1})	$\dot{\varepsilon}_B$ (10^{-7} s^{-1})	$\dot{\varepsilon}_{PL}$ (10^{-7} s^{-1})	J_{PL0} (10^{-3} MPa^{-1})	J_{PL1} (10^{-4} $MPa{\cdot}s^{-n_{MC}}$)
PCL	–	–	0.02	452 ± 66	2.11	0.26	0.11	2.46	377	2959	385	3.0	10.8	8.5	7.4	15.7	2.03	5.38
5.0MMT	Bad	Low	0.05	624 ± 40	1.97	0.19	0.04	2.18	427	2959	300	6.1	4.1	3.5	3.3	5.8	1.97	4.04
5.0C30B	Good	High	0.32	767 ± 61	1.55	0.39	0.15	2.06	508	2560	353	1.9	23.1	9.9	10.0	23.9	0.74	8.63

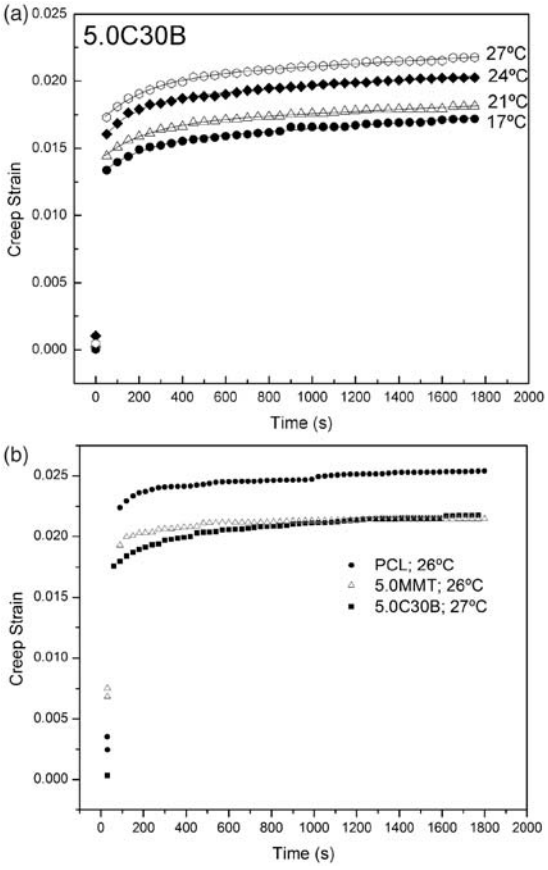

Figure 5. Creep strain as a function of time: (a) 5.0C30B at different temperatures: points represents the experimental values and lines the Burgers model fitting and (b) all systems at one temperature.

higher. Instantaneous deformation, primary, and secondary creep stages can be observed in the previous figures; whereas, there is no evidence of tertiary creep; since it would have required longer times. The comparison of the creep curves at one temperature for the three systems can be observed in Figure 5(b). It is clear from this figure that the primary and secondary creep behaviors of the organo-clay nanocomposite are quite different than those of the other systems. On the other hand, it can be also observed that this nanocomposite displayed the most effective elastic enhancement. Therefore, the behavior at each creep stage (including the elastic component) will be further analyzed. Figure 6(a)–(d) shows the instantaneous strain, ε_0 (Figure 6 (a)), the time-dependent deformations, $(\varepsilon_1-\varepsilon_0)$ (Figure 6(b)) and $(\varepsilon_2-\varepsilon_1)$ (Figure 6(c)), and the final strain, (after 30 min of applied stress: $\varepsilon_f=\varepsilon_2$ (Figure 6 (d))), for the neat PCL and nanocomposites as a function of temperature. The parameters obtained at room temperature are also reported in Table 2. The 5.0C30B nanocomposite showed the lowest ε_0 value with a

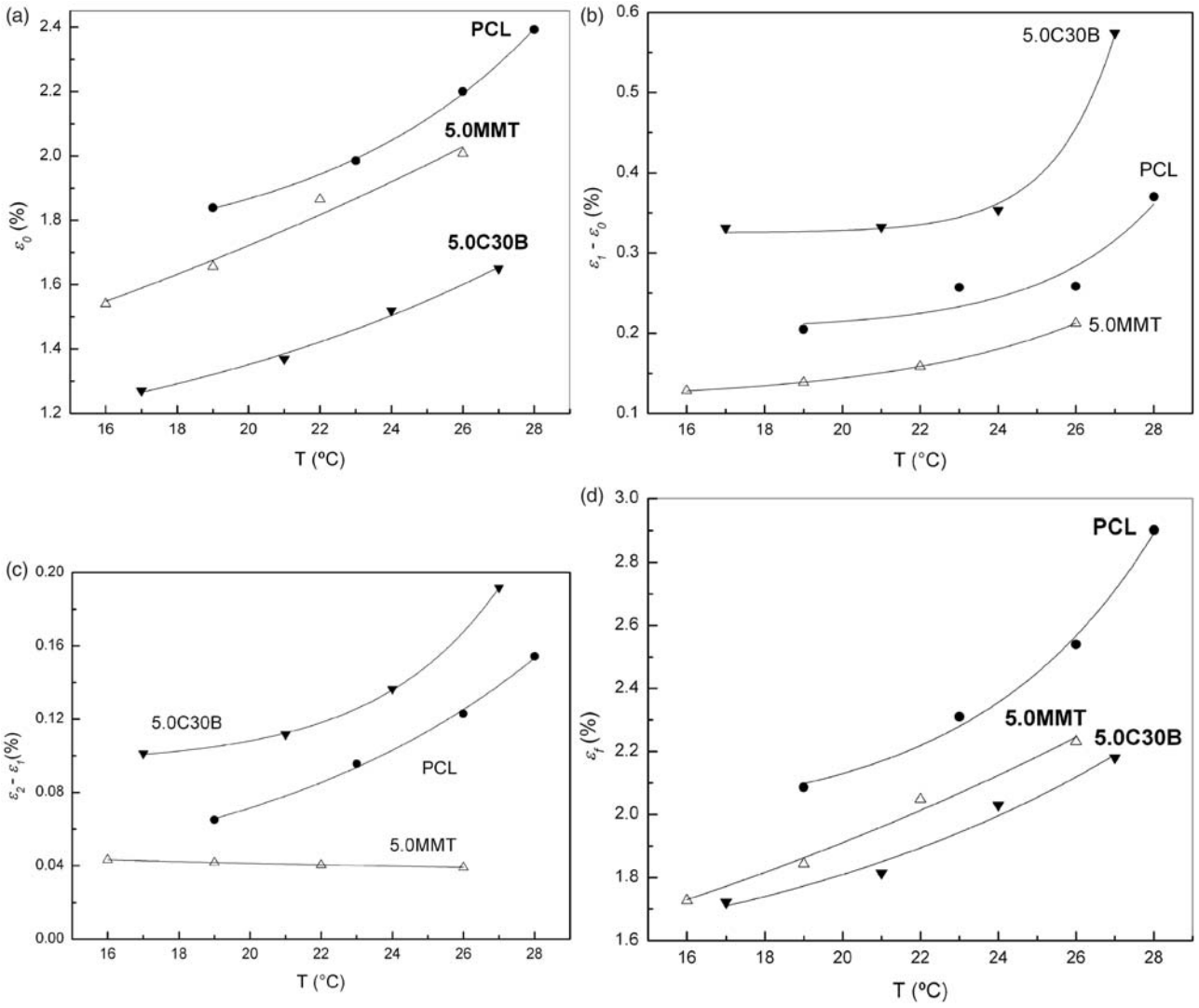

Figure 6. Experimental creep parameters as a function of the temperature for PCL and nanocomposites: (a) instantaneous strain, ε_0, (b) primary creep strain, $(\varepsilon_1 - \varepsilon_0)$, (c) secondary creep strain, $(\varepsilon_2 - \varepsilon_1)$, and (d) final creep strain, ε_f.

reduction of 24% with respect to pure PCL. It is clear the enhancement of the elastic part when clay was incorporated to the neat matrix; in addition, this improvement was more effective for well-dispersed nanocomposites. This result is also reflected on the experimental Young's modulus values which showed the same tendency. Clay dispersion plays a crucial role on the improvement of the elastic behavior of the polymeric matrix.[3,34–36] On the other hand, the viscous or time-dependent deformations, $(\varepsilon_1 - \varepsilon_0)$ and $(\varepsilon_2 - \varepsilon_1)$, followed the opposite behavior. The less dispersed nanocomposite (5.0MMT) showed the lowest values of viscous deformations and the largest instantaneous deformation ε_0 in comparison with 5.0C30B nanocomposite at all temperatures analyzed. When the ε_0 value is high, higher amounts of polymer segments are oriented along the stress direction almost instantaneously. This phenomenon can generate orientational hardening which has a crucial influence on the primary creep strain since it could make much more difficult the reorientation and rearrangement of the polymeric chains.[37] This phenomenon may also inhibit the deformation mechanisms for the irrecoverable creep strain where the damage of crystalline- and noncrystalline-oriented regions and the irreversible deformation of amorphous regions take place.[37] This hypothesis could be also applied to compare pure PCL and 5.0C30B nanocomposite. On the other hand, 5.0MMT nanocomposite showed lower ε_0, $(\varepsilon_1 - \varepsilon_0)$ and $(\varepsilon_2 - \varepsilon_1)$ values than neat PCL. The elastic behavior was improved by

MMT incorporation; thus, according to the previous hypothesis, $(\varepsilon_1 - \varepsilon_0)$ and $(\varepsilon_2 - \varepsilon_1)$ might be higher than the values for the neat matrix. In this case, two mechanisms may be competing in primary and secondary creep stages:

1. Orientational hardening of neat PCL.
2. Inhibition of amorphous polymer chains movement by MMT incorporation.

The second one may be the predominant mechanism that explains the observed behavior (comparing 5.0MMT and PCL). When comparing 5.0C30B and PCL, the difference on the elastic behavior was so high that the first mechanism became the governing one. In order to analyze this hypothesis, it is also important to know the effect of clay on the crystallinity degree of the matrix, but no important differences on this parameter were found for the studied systems.[32] Glass transition temperature (T_g) is another factor that could drastically change the viscous deformation behavior of the pure polymer, but this parameter was not affected by used clays.

From the previous analysis, we can conclude that the time-dependent deformation is strictly related to the instantaneous elastic behavior, and consequently, to the clay dispersion degree, and clay content inside the matrix.

In the case of ε_f the tendency was in accordance with that of ε_0. This is evidence that the nanoparticles have more influence on the elastic than on the time-dependent behavior of PCL matrix.

All these parameters (ε_0, $(\varepsilon_1 - \varepsilon_0)$, $(\varepsilon_2 - \varepsilon_1)$, and ε_f) seem to follow an exponential growth dependence with the temperature. An exception was observed for $(\varepsilon_2 - \varepsilon_1)$ of the 5.0MMT nanocomposite because this material does not show secondary creep strain dependence on temperature, which indicates that the movement of amorphous polymer chains is being inhibited by the presence of MMT clay as it was previously stated.

Creep behavior modeling

Four-element model. Figure 5 also includes the fitting curves (four-element model) for the 5.0C30B nanocomposite. In order to obtain accurate fitting parameters, high-quality initial values are needed, which can be obtained from the relationships between the experimental deformations and the parameters of each element of the model established in Figure 2(b).

Figure 7(a) shows E_1 values (Equation (3)) for the matrix and nanocomposites as a function of the temperature; a decreasing linear trend was observed in all cases. The linear regression of the experimental values is also included in the figure. The slopes are quite similar for all materials probably because the clay morphology is not changed in the temperature interval analyzed. Otherwise, it is evident that nanocomposites have higher E_1 values than those of the matrix (and higher when the dispersion degree was improved), this result is a direct indication of the improvement in the elastic properties. The clay surface modification led to the enhancement of the matrix/clay compatibility and thus to the best elastic performance.[21,22] Similar trends about the elastic response of the different materials were obtained either by creep tests as by static studies. Pérez et al.[22] have demonstrated for PCL/starch blends and its nanocomposites with organo-modified layered silicates that the creep compliance decreased by the incorporation of clay relating this effect with the enhancement of the elastic modulus, confirming this trend by means of E_1 (Burgers model).

Figure 7(b) and (c) shows the dependence of E_2 and τ_2 with the temperature, respectively. E_2 follows a decreasing trend with the temperature for all materials; similar results were previously obtained for similar systems.[22] The obtained behavior may arise from the fact that the polymer chains can be easily moved as far as the test temperature is further away from the glass transition temperature (T_g). The retardation time, τ_2, for PCL and 5.0C30B increased while for 5.0MMT seems to decrease with temperature. Regarding E_2 and τ_2 for PCL and 5.0C30B, it can be concluded that there was no reinforcement effect in the Kelvin unit for the nanocomposite since both parameters were lower than that of the neat matrix. These results are in accordance with the experimental behavior; observed from $(\varepsilon_1 - \varepsilon_0)$. In the case of 5.0MMT, E_2 was higher than pure PCL which goes with experimental analysis but τ_2 does not. In order to analyze the effect of the clay on the secondary creep, both parameters have to be simultaneously analyzed. In this case, the increment on E_2 may be the key parameter that conduct to a decrease on the strain in the Kelvin unit when is compared with PCL, which is in accordance with the experimental results.

Instantaneous and recoverable time-dependent components of the creep deformation have been discussed. The other important parameter is η_1 (which is related to irrecoverable creep strain, Figure 7(d)), which followed the same trend as $(\varepsilon_2 - \varepsilon_1)$ for different materials. As it was previously mentioned, the irrecoverable creep strain is related with the damage of crystalline- and noncrystalline-oriented regions; on the other hand, the irreversible deformation of amorphous regions and the orientational hardening may also inhibits these deformation mechanisms.[37] Thus, the lowest η_1 value was found for well-dispersed nanocomposites without showing any reinforcing effect on the

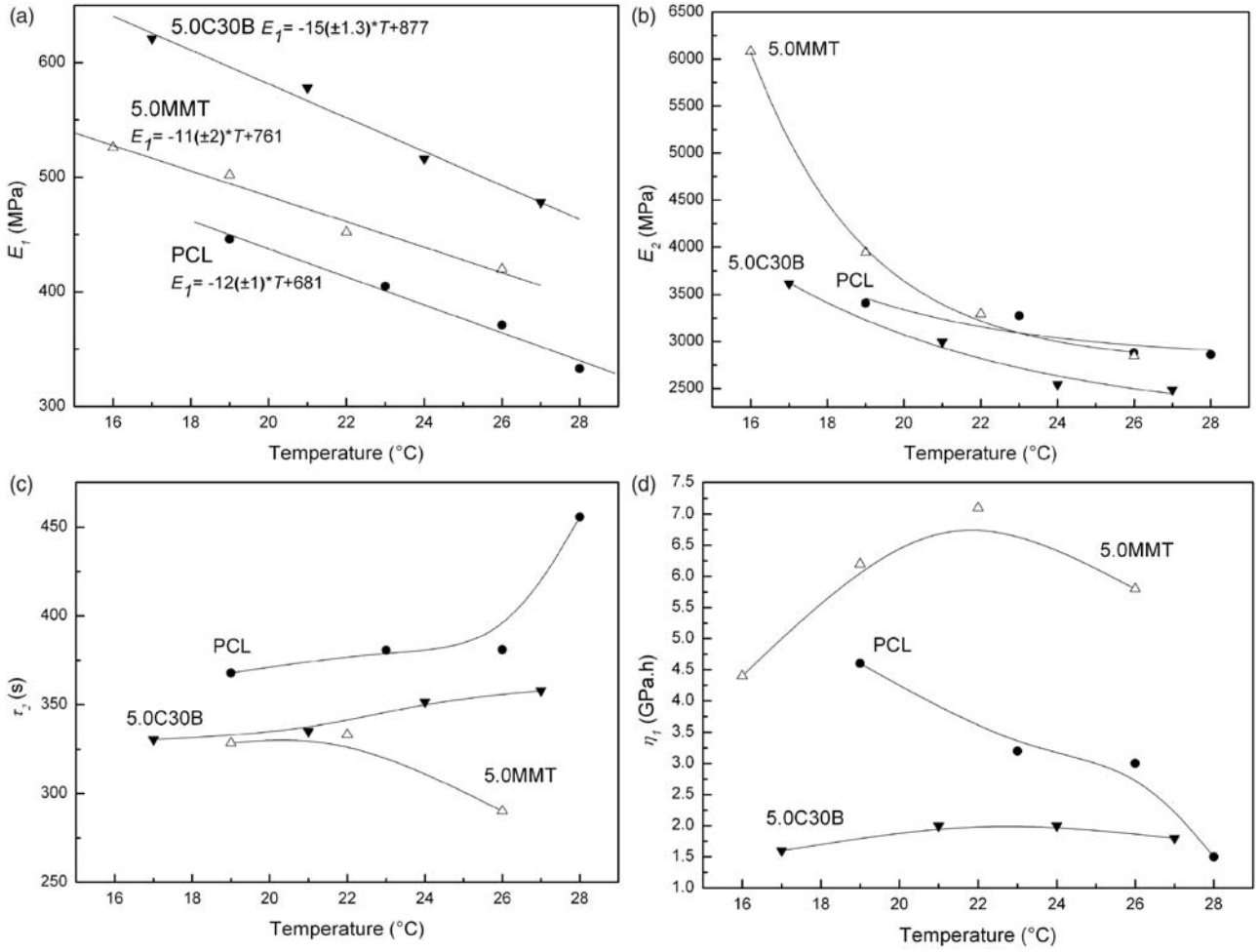

Figure 7. Parameters of the Burgers model for matrix and nanocomposites as a function of temperature: (a) elastic moduli of the Maxwell spring, E_1, (b) elastic moduli of the Kelvin–Voight unit, E_2, (c) retardation time in the Kelvin–Voight unit, τ_2, and (d) viscosity of the Maxwell dashpot, η_1.

irrecoverable creep strain. From Figure 7(d), it can be observed that η_1 does not follow a clear tendency with temperature.

From Table 2, it can be observed that all elastic parameters (static, experimental, and modeled creep ones) are in accordance with the clay dispersion degree. Whereas better clay dispersion inside the nanocomposites improved the elastic behavior of PCL, it led to higher viscous deformations. Finally, the enhancement of the elastic part was so high in the case of well-dispersed nanocomposites that the overall creep behavior was improved.

Findley power law model

Findley power law is an easily applicable model that has been widely used to predict long-term creep properties of polymers.[30] A good correlation between the fitting curves (model) and the experimental points was

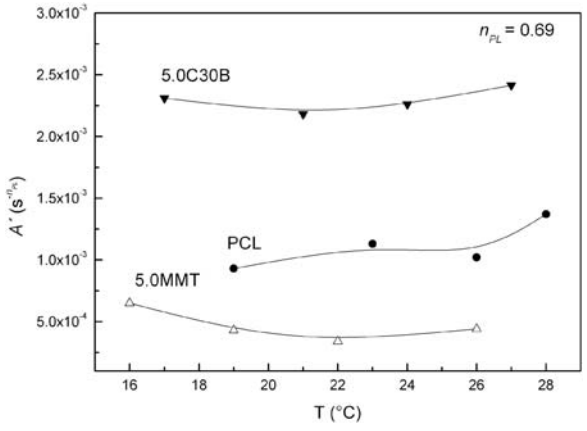

Figure 8. Effect of temperature and clay type on the amplitude of transient creep strain (A') obtained by the Findley power law model; $n_{PL} = 0.69$.

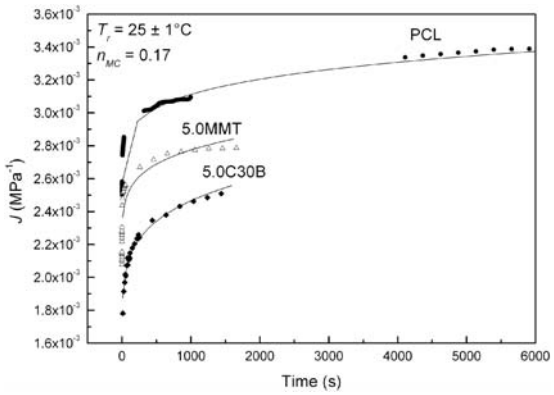

Figure 9. Master curves and Findley power law fitting for PCL and nanocomposites; $T_r = 25°C \pm 1°C$ and n_{MC}.

obtained. In a first approach A' and n_{PL} parameters from Equation (5) were modeled; it was found that n_{PL} did not change either with temperature or by clay incorporation, so that a fixed n_{PL} value ($n_{PL} = 0.69$) was used for fitting. This assumption allowed us to obtain better understanding on the A' behavior. Figure 8 shows the dependence of A' with the temperature for PCL and nanocomposites (Table 2 also includes A' at 25°C). A significant dependence of A' with the temperature was not observed. It could be related to the fact that A' includes the instantaneous creep strain by $A' = A/\varepsilon_0$ so that, even when A increased with temperature, ε_0 also does it leading to almost constant values. A' (related with the experimental viscous behavior) showed the same trend for different materials than the time-dependent experimental behavior (measured by $(\varepsilon_1 - \varepsilon_0)$ and $(\varepsilon_2 - \varepsilon_1)$) and the viscous Burgers parameters (E_2, τ_2, and η_1), except to τ_2 value for 5.0MMT. Regarding the viscous deformation, once again, it is demonstrated that the well-dispersed nanocomposites do not act as reinforcement showing the opposite behavior of elastic parameters.

Creep rates

As it was previously demonstrated, the power law (Findley) and also the four-element model (Burger) were suitable to reproduce the strain as a function of time data. Besides the parameters of each model, another characteristic and interesting factor is the creep rate, which also determines the dimensional stability of materials. Table 2 shows a comparison between the experimental (calculated from the slope of the linear strain–time region in the secondary creep stage) and model-derived creep rates at 25°C for the different materials analyzed in this study. All parameters showed the same tendency. Only the 5.0MMT nanocomposite displayed lower creep rate than that of the neat matrix; opposite, the creep rate of 5.0C30B nanocomposite was higher than that of neat PCL. These results are in accordance with the experimental viscous behavior and the time-dependent parameters (from both models) that have been previously analyzed; it was expected since creep rate is directly related to the viscous behavior (Equations (4) and (7)). It is important to note that four-element model is especially useful since not only the tendency was the same as the experimental one, but also the values were very similar.

Master curves

Figure 9 shows the master curves ($T_r = 25°C$) for matrix and nanocomposites. Table 2 includes the parameters of Equation (10) ($T_r = 25°C$, $n_{MC} = 0.1$). The shape of the curves was quite similar for all materials. The creep resistance was higher (lower J) for the nanocomposites than for neat matrix (for the analyzed time scale) and the improvement was more efficient in the case of well-dispersed nanocomposites.

Regarding the Findley power law model parameters for master curves (Table 2), it can be observed that J_{PL0} (related to the elastic behavior) was lower for well-dispersed nanocomposites, while J_{PL1} (time-dependent term) followed the opposite behavior. Once again, it is evident that good dispersion of the clay platelets leads to a great enhancement of the elastic behavior but does not improve the time-dependent performance. Whereas initially the creep resistance is higher for the nanocomposite that shows the best clay dispersion degree (related with the elastic part which predominates at short times); this tendency can be reverted at longer times as a consequence of the higher time-dependent deformations. Therefore, for applications where creep must be considered, good clay dispersion may not always enhance the creep resistance of the matrix. In future works, creep tests at longer times and a wider temperature interval will be carried out in order to validate these conclusions.

Pérez et al.[22] have shown for starch/PCL-organo-modified clay nanocomposites that the master curves displayed a tolerable superposition and the activation energy for the shift factor was also an evidence for the creep resistance development.

Conclusions

PCL/clay nanocomposites were prepared by melt processing using two different types of clays. The results of traditional techniques, such as XRD and TEM, together with the mechanical properties and melt rheology confirmed the increase on the clay dispersion degree when montmorillonite was organo-modified

due to the enhancement of the polymer/clay compatibility.

Regarding creep behavior, it was found that original and modified clays acted as reinforcement enhancing the creep resistance of the neat matrix, but the creep resistance was better when clay dispersion degree was improved. What is remarkable is that this improvement was strictly related to the enhancement of the elastic behavior since the time-dependent analysis revealed the opposite tendency.

Four-parameter and power law models correctly correlated the experimental deformation data of all materials. The variation of the parameters obtained illustrated the effect of nanoclays on the creep performance. The quality of the master curve was acceptable and could be modeled by the Finley power law.

All results give the idea that to design a material for a given application in which a load is applied continuously over a period of time, the time-dependent deformation becomes relevant for well-dispersed nanocomposites and the enhancement of the creep resistance found at short times could be reverted when long-term analysis is performed.

Funding

The authors acknowledge 'Agencia Nacional de Promoción Científica y Tecnológica, ANPCyT (PICT06 1560)' for the financial support of this project.

References

1. Lepoittevin B, Devalckenaere M, Pantoustier N, Alexandre M, Kubies D, Calberg C, et al. Poly(ε-caprolactone)/clay nanocomposites prepared by melt intercalation: mechanical, thermal and rheological properties. *Polymer* 2002; 43(14): 4017–4023.
2. Kuniok M, Ninomiya F and Funabashi M. Novel evaluation method of biodegradabilities for oil-based polycaprolactone by naturally occurring radiocarbon-14 concentration using accelerator mass spectrometry based on ISO 14855-2 in controlled compost. *Polym Degrad Stab* 2007; 92(7): 1279–1288.
3. Ludueña LN, Alvarez VA and Vazquez A. Processing and microstructure of PCL/clay nanocomposites. *Mater Sci Eng A* 2007; 460–461: 121–129.
4. Messersmith PB and Giannelis EP. Synthesis and barrier properties of poly(ε-caprolactone)-layered silicate nanocomposites. *J Polym Sci Part A: Polym Chem* 1995; 33(7): 1047–1057.
5. Kojima Y. Usuki A, Kawasumi M, Okada A, Fukushima Y, Jurauchi T, et al., Mechanical properties of nylon 6-clay hybrid. *J Mater Res* 1993; 8(5): 1185–1189.
6. Gilman J, Jackson C, Morgan A, Harris R, Manias E, Giannelis E, et al. Flammability properties of polymer−layered-silicate nanocomposites polypropylene and polystyrene nanocomposites. *Chem Mater* 2000; 12(7): 1866–1873.
7. Gorrasi G, Tortora M, Vittoria V, Pollet E, Lepoittevin B, Alexandre M, et al. Vapor barrier properties of polycaprolactone montmorillonite nanocomposites: effect of clay dispersion. *Polymer* 2003; 44(8): 2271–2279.
8. Zhang Z, Yang JL and Friedrich K. Creep resistant polymeric nanocomposites. *Polymer* 45(10): 3481–3485.
9. Maiti P. Influence of miscibility on viscoelasticity, structure, and intercalation of oligo-poly(caprolactone)/layered silicate nanocomposites. *Langmuir* 2003; 19(13): 5502–5510.
10. Hartmut F. Polymer nanocomposites: from fundamental research to specific applications. *Mater Sci Eng C* 2003; 23(6–8): 772.
11. Alexandre M and Dubois P. Polymer-layered silicate nanocomposites: preparation, properties and uses of a new class of materials. *Mater Sci Eng: R* 2000; 28(1–2): 1–63.
12. Manitiu M, Horsch S, Gulari E and Kannan RM. Role of polymer–clay interactions and nano-clay dispersion on the viscoelastic response of supercritical CO2 dispersed polyvinylmethylether (PVME)–Clay nanocomposites. *Polymer* 2009; 50(15): 3786–3796.
13. Ray S and Okamoto M. Polymer/layered silicate nanocomposites: a review from preparation to processing. *Prog Polym Sci* 2003; 28(11): 1539–1641.
14. Krishnamoorti R, Vaia RA and Giannelis EP. Structure and dynamics of polymer-layered silicate nanocomposites. *Chem Mater* 1996; 8(8): 1728–1734.
15. Zhao J, Morgan AB and Harris JD. Rheological characterization of polystyrene–clay nanocomposites to compare the degree of exfoliation and dispersion. *Polymer* 2005; 46(20): 8641–8660.
16. Sung L, Chung L, Hyoung C and Myung J. Solidlike transition of melt-intercalated biodegradable polymer/clay nanocomposites. *J Polym Sci: Part B Polym Phys* 2003; 41: 2052–2061.
17. Wagener R and Reisinger TJG. A rheological method to compare the degree of exfoliation of nanocomposites. *Polymer* 2003; 44(24): 7513–7518.
18. Yang JL, Zhang Z, Schlarb AK and Friedrich K. On the characterization of tensile creep resistance of polyamide 66 nanocomposites. Part II: modeling and prediction of long-term performance. *Polymer* 2006; 47: 6745–6758.
19. Pegoretti A, Kolarik J, Peroni C and Migliaresi C. Recycled poly(ethylene terephthalate)/layered silicate nanocomposites: morphology and tensile mechanical properties. *Polymer* 45(8): 2751–2759.
20. Galgali G, Ramesh C and Lele A. A rheological study on the kinetics of hybrid formation in polypropylene nanocomposites. *Macromolecules* 2001; 34(4): 852–858.
21. Ranade A, Nayak K, Fairbrother D and D'Souza NA. Maleated and non-maleated polyethylene–montmorillonite layered silicate blown films: creep, dispersion and crystallinity. *Polymer* 2005; 46(18): 7323–7333.
22. Pérez J, Alvarez VA and Vazquez A. Creep behaviour of layered silicate/starch–polycaprolactone blends nanocomposites. *Mater Sci Eng A* 2008; 480(1–2): 259–265.
23. Chiou BS, Yee E, Glenn G and Orts W. Rheology of starch–clay nanocomposites. *Carbohydr Polym* 2005; 59(4): 467–475.

24. Krishnamoorti R, Ren J and Silva AS. Shear response of layered silicate nanocomposites. *J Chem Phys* 2001; 114(11): 4968–4973.
25. Durmus A, Kasgoz A and Macosko CW. Linear low density polyethylene (LLDPE)/clay nanocomposites. Part I: structural characterization and quantifying clay dispersion by melt rheology. *Polymer* 2007; 48(15): 4492–4502.
26. ASTM D 2990-01. *Standard test methods for tensile, compressive, and flexural creep and creep-rupture of plastics*. West Conshohocken: ASTM International, 2001.
27. Schapery RA. Nonlinear viscoelastic and viscoplastic constitutive equations based on thermodynamics. *Mech Time-Depend Mater* 1(2): 209–240.
28. Nielsen LE and Landel RF. *Chapter 3: creep and stress relaxation, mechanical properties of polymers and composites*, 2nd ed. New York: Marcel Dekker, Inc, 1994, pp.63–68.
29. Rosen SL. *Chapter 18: linear viscoelasticity, fundamental principles of polimeric materials*, 2nd ed. New York: John Wiley & Sons, Inc, 1993, pp.307–309.
30. Findley WN, Lai JS and Onaran K. *Chapter 2: historical survey of creep, creep and relaxation of nonlinear viscoelastic materials: with an introduction to linear viscoelasticity*. New York: Dover Publications, Inc, 1989, pp.13–17.
31. Williams ML, Landel RF and Ferry JD. The temperature dependence of relaxation mechanisms in amorphous polymers and other glass-forming liquids. *J Am Chem Soc* 1955; 77: 3701–3707.
32. Ludueña LN, Vázquez A and Alvarez VA. Crystallization of polycaprolactone-clay nanocomposites. *J Appl Polym Sci* 109(5): 3148–3156.
33. Dennis HR, Hunter DL, Chang D, Kim S, White JL and Cho JW. Effect of melt processing conditions on the extent of exfoliation in organoclay-based nanocomposites. *Polymer* 2001; 42(23): 9513–9522.
34. Lee DC and Jang LE. Preparation and characterization of PMMA-Clay hybrid composite by emulsion polymerization. *J Appl Polym Sci* 1996; 61(7): 1117–1122.
35. Noh MW and Lee DC. Synthesis and characterization of PS-clay nanocomposite by emulsion polymerization. *Polym Bull* 1999; 42(5): 619–626.
36. Hasegawa N, Kawasumi M, Kato M, Usuki A and Okada A. Preparation and mechanical properties of polypropylene-clay hybrids using a maleic anhydride-modified polypropylene oligomer. *J Appl Polym Sci* 1998; 67(1): 87–92.
37. Harren SV. Toward a new phenomenological flow rule for orientationally hardening glassy polymers. *J Mech Phys Solids* 2003; 43(7): 1151–1173.